

BLOOD-BASED BIOMARKERS

Plasma pyroglutamate-modified amyloid beta differentiates amyloid pathology

Pei-Ning Wang^{1,2,3} | Kun-Ju Lin^{4,5} | Huei-Chun Liu⁶ | Ulf Andreasson^{7,8} |
Kaj Blennow^{7,8} | Henrik Zetterberg^{7,8,9,10} | Shieh-Yueh Yang^{6,11}

¹Department of Neurology, Neurological Institute, Taipei Veterans General Hospital, Taipei, Taiwan

²Department of Neurology, School of Medicine, National Yang-Ming University, Taipei, Taiwan

³Brain Research Center, National Yang-Ming University, Taipei, Taiwan

⁴Department of Nuclear Medicine and Molecular Imaging Center, Linkou Chang Gung Memorial Hospital, Tao-Yuan, Taiwan

⁵Healthy Aging Research Center and Department of Medical Imaging and Radiological Sciences, College of Medicine, Chang Gung University, Tao-Yuan, Taiwan

⁶MagQu Co., Ltd., New Taipei City, Taiwan

⁷Department of Psychiatry and Neurochemistry, Institute of Neuroscience and Physiology, the Sahlgrenska Academy at the University of Gothenburg, Mölndal, Sweden

⁸Clinical Neurochemistry Laboratory, Sahlgrenska University Hospital, Mölndal, Sweden

⁹Department of Neurodegenerative Disease, UCL Queen Square Institute of Neurology, Queen Square, London, UK

¹⁰UK Dementia Research Institute at UCL, London, UK

¹¹MagQu LLC, Surprise, Arizona, USA

Correspondence

Shieh-Yueh Yang, MagQu Co., Ltd., New Taipei City 231, Taiwan.
E-mail: syyang@magqu.com

Funding information

Swedish Research Council, Grant/Award Number: #2017-00915; Swedish Alzheimer Foundation, Grant/Award Number: #AF-742881; Hjärfonden, Sweden, Grant/Award Numbers: #FO2017-0243, #ALFGBG-715986

Abstract

Introduction: Pyroglutamate-modified amyloid β ($A\beta_{pE3}$) could be a biomarker for $A\beta$ plaque pathology in the brain. An ultra-high-sensitive assay is needed for detecting $A\beta_{pE3-40}$.

Methods: Immunomagnetic reduction was used for quantification of $A\beta_{pE3-40}$ in plasma from 46 participants. The concentrations of $A\beta_{pE3-40}$ of these subjects were compared with ¹⁸F-florbetapir positron emission tomography (PET) images.

Results: $A\beta_{pE3-40}$ concentration was 44.1 ± 28.2 fg/mL in PET- ($n = 28$) and 91.6 ± 54.6 fg/mL in PET+ ($n = 18$; $P < .05$). The cutoff value of $A\beta_{pE3-40}$ for discriminating PET- from PET+ was 55.5 fg/mL, resulting in a sensitivity of 83.3%, a specificity of 71.4%. The concentration of $A\beta_{pE3-40}$ showed a moderate correlation ($r = 0.437$) with PET standardized uptake value ratio.

Discussion: We did not enroll pre-clinical AD subject with normal cognition but $A\beta$ PET+. It would be an important issue to explore the feasibility of using $A\beta_{pE3-40}$ for screening pre-clinical subjects.

Conclusion: These results reveal the feasibility of detecting $A\beta$ pathology using quantification of a plaque-derived $A\beta$ molecule in plasma.

This is an open access article under the terms of the Creative Commons Attribution-NonCommercial License, which permits use, distribution and reproduction in any medium, provided the original work is properly cited and is not used for commercial purposes.

© 2020 The Authors. *Alzheimer's & Dementia: Diagnosis, Assessment & Disease Monitoring* published by Wiley Periodicals, Inc. on behalf of the Alzheimer's Association.

1 | INTRODUCTION

Amyloid β ($A\beta$) aggregation in the brain is the pathological hallmark of Alzheimer's disease (AD).¹⁻⁴ Toxic effects of these $A\beta$ aggregates are correlated with the predominance of N-terminally truncated species over the full-length $A\beta$.⁵⁻⁷ Using mass spectrometry, various types of N-terminally truncated species of $A\beta_{n-40/42}$ are found in AD brain tissue, including N-terminally truncated $A\beta_{3-40/42}$ that have been further catalyzed by glutaminyl cyclase to form pyroglutamate $A\beta$ cyclization ($A\beta_{pE3}$) variants.⁸⁻¹⁰ The particular $A\beta$ form has high toxicity, high resistance to proteolytic degradation, increased hydrophobicity, and faster aggregation.^{7,11-13} Thus, $A\beta_{pE3}$ may be an important culprit during AD initiation and progression.

$A\beta_{pE3}$ is evidenced as a major constituent of intra-/extracellular and vascular $A\beta$ deposits in AD brain tissue.¹⁴⁻¹⁶ In addition to *post mortem* human brain tissues, the abnormal levels of $A\beta_{pE3}$ in the brain and the co-localization of $A\beta_{pE3}$ with $A\beta$ plaques were found in different animal models, such as transgenic mice, canines, and Caribbean vervets.¹⁷⁻¹⁹ These results suggest that $A\beta_{pE3}$ is a potential seeding species and may play an important role in the formation of pathological $A\beta$ aggregates in the brain.^{14,20} It could also be a biomarker specific for $A\beta$ plaque pathology in the brain.²¹

So far, the reported evidence for finding abnormal amyloidosis by $A\beta_{pE3}$ in AD is tissues of animals or *post mortem* human brains. The difficulties of obtaining human brain samples seriously limit the exploration of $A\beta_{pE3}$ in clinical cohorts. It is believed that the measurement $A\beta_{pE3}$ in body fluids such as plasma would be important to further explore the relevance of $A\beta_{pE3}$ in AD pathogenesis, and plasma $A\beta_{pE3}$ may also have a potential as a diagnostic tool in the clinic. However, the concentration of $A\beta_{pE3}$ in human body fluid is extremely low. An ultra-high-sensitive assay technology is needed for detecting $A\beta_{pE3}$ in human body fluids.

Immunomagnetic reduction (IMR) is an ultra-sensitive technology for assaying biomarkers at pg/mL or lower.^{22,23} In addition, the correlation between these plasmas biomarkers and their concentration in cerebrospinal fluid (CSF),²⁴ and their relation to neuroimaging measures such as $A\beta$ positron emission tomography (PET) have been clarified.^{25,26} The results reveal the reliabilities of assaying ultra-low-concentrated biomarkers using IMR. In this work, IMR was used to develop the quantitative detection of $A\beta_{pE3-40}$ in human plasma. Moreover, 28 subjects with negative $A\beta$ PET (PET-) and 18 subjects with positive $A\beta$ PET (PET+) were enrolled. The measured concentrations of plasma $A\beta_{pE3-40}$ of these subjects were compared with amyloid PET. Moreover, the plasma $A\beta_{1-40}$ of all subjects were assayed using an IMR $A\beta_{1-40}$ kit to explore the roles of $A\beta_{1-40}$ and $A\beta_{pE3-40}$ in discriminating $A\beta$ PET status.

Research in Context

1. Pyroglutamate-modified amyloid β ($A\beta_{pE3}$) is a modified $A\beta$ peptide that co-oligomerizes with $A\beta_{42}$ and deposited in the Alzheimer's disease (AD) brain. $A\beta_{pE3}$ may act as a seed for misfolding of $A\beta$ at a primary step in AD. The concentration of $A\beta_{pE3}$ in body fluid is extremely low. Therefore, an ultra-sensitive assay such as immunomagnetic reduction assay is developed to detect the level of $A\beta_{pE3}$ in plasma.
2. We developed a new analysis method to measure the concentration of $A\beta_{pE3}$. This study demonstrates the plasma $A\beta_{pE3-40}$ showed a correlation with $A\beta$ positron emission tomography (PET) status and standardized uptake value ratio, which may be of value for screening and diagnosis as well as for applications in longitudinal clinical research studies and to monitor treatments in clinical trials.
3. Detection of plasma $A\beta_{pE3-40}$ in early stages could be a potential strategy for early diagnosis of AD. However, more participants should be enrolled for validating the correlation between $A\beta_{pE3-40}$ and $A\beta$ PET status.

2 | METHODS

2.1 | IMR reagent for assaying $A\beta_{pE3-40}$

Antibodies against $A\beta_{pE3-40}$ were developed by Biogen Inc. According to the results via direct binding enzyme-linked immunosorbent assay (ELISA), the antibodies show strong reactivity to $A\beta_{pE3-40}$ and $A\beta_{3-40}$ (>0.3 nM), and weak reactivity to $A\beta_{1-40}$, but not $A\beta_{pE11-40}$. There is not any available data concerning the reactivity with $A\beta_{pE3-42}$. Antibodies against $A\beta_{pE3-40}$ were covalently bound to dextran-coated Fe_3O_4 nanoparticles (MF-DEX-0060, MagQu) via the chemical reactions in Yang et al.²⁷

2.2 | IMR measurements

The IMR analyzer (XacPro-S, MagQu) was used to detect the reduction in the magnetic signals of reagent due to the association between antibody-functionalized magnetic nanoparticles and $A\beta_{pE3-40}$ molecules. The ratio of the reduction to the alternative-current magnetic signal of reagent before incubation is referred as IMR signal, as expressed

$$\text{IMR} (\%) = \frac{\chi_{ac,o} - \chi_{ac,\phi}}{\chi_{ac,o}} \times 100\%, \quad (1)$$

where $\chi_{ac,o}$ and $\chi_{ac,\phi}$ are the alternative-current magnetic signals of reagent before and after incubation. For each reported IMR (%) in this work, an averaged value of duplicated IMR measurements was used.

2.3 | Recruitment of subjects

All subjects were recruited in the study of the Alzheimer's Disease Neuroimaging Initiative at Taipei Veterans General Hospital (Taipei VGH), Linkou Chang Gung Memorial Hospital (CGMH), and Kaohsiung CGMH in Taiwan (T-ADNI). The T-ADNI study was approved by the ethics committees of the three hospitals. All participants were asked to complete written informed consents for this study.

Enrolled subjects were required to be aged >55 years. Magnetic resonance imaging (MRI) was used to exclude subjects with major neuropathologies such as tumors, strokes, severe white matter disease, or inflammation, but MRI was not used to diagnose dementia. Subjects with history of major brain trauma, stroke, brain tumor, epilepsy, major psychiatric illness, alcoholism, or other systemic diseases that might affect cognitive function were ruled out in this study.

The study included a battery of neuropsychological tests including the Geriatric Depression Scale, a Mini-Mental State Examination (MMSE), and the Chinese version of the Wechsler Memory Scale-III (WMS-III). A Clinical Dementia Rating Scale (CDR) score was performed for each enrolled subject. Patients with AD and amnesic mild cognitive impairment (aMCI) patients follows criteria of National Institute on Aging and the Alzheimer's Association (NIA-AA).²⁸

2.4 | Collection and preparation of human plasma samples

Each enrolled subject provided a 9 mL non-fasting venous blood sample (K3 ethylenediaminetetraacetic acid [EDTA], lavender-top tube). Blood samples were centrifuged at 1500 to 2500 × g at room temperature for 15 minutes within 1 hour after blood draw. Plasma was then aliquoted into cryotubes (0.5 mL aliquots) and stored at -20°C.

2.5 | Analysis of apolipoprotein E (APOE) genotypes

APOE genotyping was performed for each enrolled subject by polymerase chain reaction (PCR) amplification of a 500 base-pair fragment of the APOE gene spanning the bases coding for amino acid positions 112 and 158, followed by direct DNA sequencing.²⁹ Subjects with either one or two ε4 alleles were regarded as ε4 carriers.

2.6 | Aβ PET imaging

All PET images were acquired from Linkou Chang Gung Memorial Hospital. The details of Aβ PET imaging were described in Lin et al. and

Hsiao et al.^{30,31} The ¹⁸F-florbetapir PET scan comprised a 10-minute acquisition period (acquired in 2 × 5-minute frames) beginning 50 minutes following 10 mCi injection of the ¹⁸F-florbetapir tracer. Imaging was performed on a Biograph mCT PET/CT scanner (GE Healthcare, Milwaukee, WI, USA). Structural MRI scans were acquired using a uniform scanning protocol that minimized and accounted for between-site differences in MRI systems.

All PET image data were processed and analyzed using PMOD image analysis software (version 3.7, PMOD Technologies Ltd., Zurich, Switzerland), including MR-based spatial normalization to the Montreal Neurological Institute (MNI) MRI template. Seven volumes of interest (VOIs), the frontal, anterior cingulate, posterior cingulate, precuneus, parietal, occipital, and temporal areas, were selected, and the regional standardized uptake value ratio (SUVR) using the whole cerebellum as the reference region was calculated for each VOI. Moreover, the average SUVR from these seven cerebral cortical VOIs was computed to yield an estimate of global cortical SUVR for further analysis.

The PET images were interpreted blindly by an experienced nuclear medicine physician (Kun-Ju Lin). A five-point visual scale was used to classify the amyloid loading, from 0, indicated no tracer retention in cortical gray matter, to 4, indicated high levels of cortical amyloid accumulation. Visual rating scores of 2 to 4 were considered indicative of amyloid PET+ brains and ratings of 0 to 1 were considered negative for amyloid PET.³²

2.7 | Assay of plasma Aβ₁₋₄₀

IMR reagent for Aβ₁₋₄₀ (MF-AB0-0060, MagQu) with an aid of IMR analyzer (XacPro-S, MagQu) were used to detect the concentrations of plasma Aβ₁₋₄₀ of subjects. Duplicated measurements were done for each sample. The reported concentration of the plasma Aβ₁₋₄₀ is the mean value of the duplicated measurements. The variations of measured concentrations of control solutions with respect to the known concentrations should be <15%.

2.8 | Statistical methods

Continuous variables for each measurement are presented as means ± standard deviations. Continuous variables were compared using a *t*-test, and *P*-values were determined. Pearson correlation *r* was done with GraphPad Prism. Negative, positive, overall percentage agreements were calculated to quantify the consistency between plasma-biomarker diagnosis and clinical diagnosis.

3 | RESULTS

3.1 | Aβ_{pE3-40} concentration-dependent IMR(%)

Phosphate buffered saline (PBS) solutions spiked with various concentrations of Aβ_{pE3-40} from 0.1 fg/mL to 1000 pg/mL were assayed

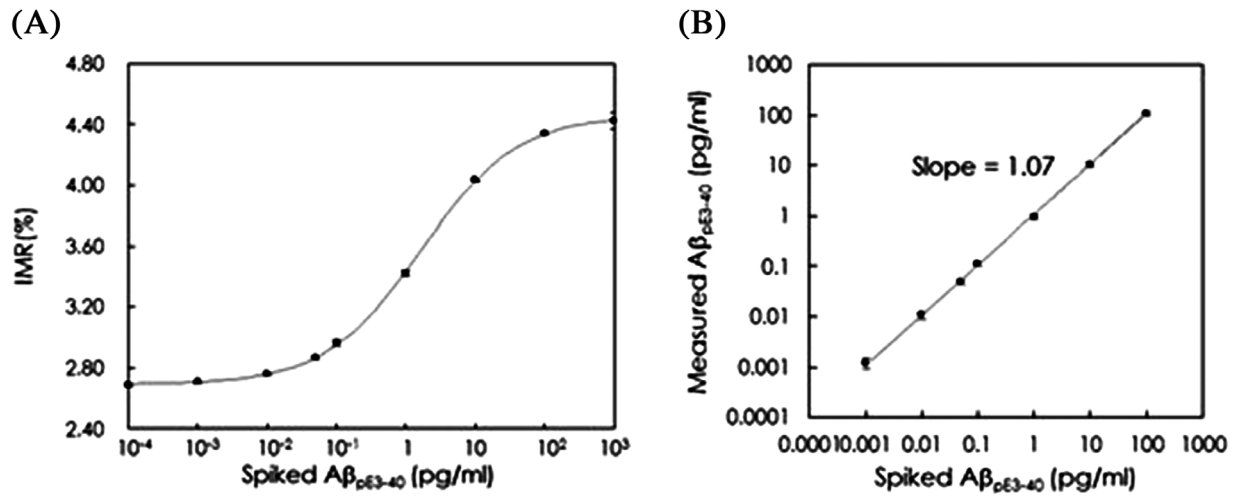


FIGURE 1 A, Amyloid β ($A\beta_{pE3-40}$) concentration-dependent IMR signals and (B) relationship between spiked concentration of $A\beta_{pE3-40}$ (x axis) and measured concentration of $A\beta_{pE3-40}$ (y axis) using immunomagnetic reduction

TABLE 1 Interference tests of $A\beta_{3-40}$, $A\beta_{1-42}$, and $A\beta_{1-40}$ for assaying $A\beta_{pE3-40}$ using immunomagnetic reduction

Sample No.	Intuition	Measured $A\beta_{pE3-40}$ concentration			Recovery rate (%)
		Mean (pg/mL)	SD (pg/mL)	CV (%)	
1	Plasma	0.0229	0.0061	26.46	-
2	Plasma + $A\beta_{pE3-40}$ (0.05 pg/mL)	0.0741	0.0051	6.83	(Ref.)
3	Plasma + $A\beta_{pE3-40}$ (0.05 pg/mL) + $A\beta_{3-40}$ (20 pg/mL)	0.0781	0.0105	13.47	105.46
4	Plasma + $A\beta_{pE3-40}$ (0.05 pg/mL) + $A\beta_{1-42}$ (20 pg/mL)	0.0734	0.0064	8.72	99.06
5	Plasma + $A\beta_{pE3-40}$ (0.05 pg/mL) + $A\beta_{1-40}$ (80 pg/mL)	0.0776	0.0089	11.45	104.73
6	Plasma + $A\beta_{pE3-40}$ (0.05 pg/mL) + $A\beta_{1-40}$ (100 pg/mL)	0.0842	0.0023	2.76	113.66

Abbreviations: $A\beta$, amyloid β ; CV, coefficient of variation; SD, standard deviation

with IMR. For each concentration, duplicated IMR measurements were performed. The averaged IMR(%) of the duplicated measurement was used to establish the relationship between IMR(%) and $A\beta_{pE3-40}$ concentration. Figure 1A shows the relationship between IMR(%) and spiked $A\beta_{pE3-40}$ concentration. The error bars with each data point are attributed from the duplicated measurements. It was observed in Figure 1A that IMR(%) increased from 2.69% to 4.42% as spiked β_{pE3-40} concentration increases from 0.1 fg/mL to 1000 pg/mL. The relationship in Figure 1A follows the logistic function

$$\text{IMR} (\%) = \left[\frac{A - B}{1 + \left(\frac{\phi_{A\beta_{pE3-40}}}{\phi_0} \right)^\gamma} + B \right] \%, \quad (2)$$

where A , B , ϕ_0 , and γ are fitting parameters; $\phi_{A\beta_{pE3-40}}$ denotes the spiked $A\beta_{pE3-40}$ concentration in PBS. By fitting Equation (2) to the experimental data points in Figure 1A, the values for the parameters A , B , ϕ_0 , and γ were found to be 2.69, 4.46, 1.67, and 0.628, respectively. A in Equation (2) is the IMR(%) as the spiked $A\beta_{pE3-40}$ concentration approaches zero. Thus, A denotes the noise level for IMR(%). B in Equation (2) is the IMR(%) as the spiked $A\beta_{pE3-40}$ concentration approaches infinity. Thus, B denotes the upper-limit signal for IMR(%)

3.2 | Lower limit of detection of the $A\beta_{pE3-40}$ assay

The lower limit of detection is usually defined as the concentration showing the IMR(%) higher than the noise level by triple standard deviation for IMR signals at low concentrations. According to the results in Table 1, the standard deviation for IMR(%) at low concentrations, such as the spiked 0.001-pg/mL $A\beta_{pE3-40}$, was found to be 0.06%. Thus, the lower limit of detection in terms of IMR(%) was $(2.69 + 3 \times 0.06)\% = 2.88\%$. Via the logistic function in Equation (2), the lower limit of detection for assaying $A\beta_{pE3-40}$ using IMR was around 0.005 pg/mL, that is, 5 fg/mL.

3.3 | Measurement range of the $A\beta_{pE3-40}$ assay

The measured IMR(%) in Figure 1A was converted to the measured $A\beta_{pE3-40}$ concentration via Equation (2). The correlations between measured $A\beta_{pE3-40}$ concentrations and spiked $A\beta_{pE3-40}$ concentrations were investigated. The results are shown in Figure 1B. Notably, one of the duplicated measurements of IMR(%) for 0.1 fg/mL $A\beta_{pE3-40}$ PBS sample was $<2.69\%$, which was the noise level of IMR(%). The measured $A\beta_{pE3-40}$ concentration was not available for this IMR(%)

TABLE 2 Demographic information of enrolled subjects

Amyloid PET Dx(n)	Negative (A β PET-)				Positive (A β PET+)		
	NC(5)	aMCI(18)	AD(5)	Combined(28)	aMCI(7)	AD(11)	Combined(18)
Female/male	3/2	7/11	1/4	11/17	7/0	4/7	11/7
Age (years)	60.4 \pm 2.8	71.2 \pm 9.8	75.6 \pm 11.5	70.1 \pm 10.3	72.7 \pm 5.9	71.2 \pm 9.2	71.8 \pm 7.92
Education (years)	14.2 \pm 2.9	10.8 \pm 3.6	13.0 \pm 3.0	11.8 \pm 3.6	12.7 \pm 5.6	13.5 \pm 3.1	13.2 \pm 4.1
ApoE ϵ 4 allele frequency	30%	2.78%	0%	7.69%	7.14%	36.36%	25%
CDR	0	0.5	0.6 \pm 0.2	0.43 \pm 0.22	0.5	0.5	0.50 \pm 0.00
MMSE	29.6 \pm 0.89	27.28 \pm 2.03	24.0 \pm 3.54	27.11 \pm 2.74	26.14 \pm 2.41	22.82 \pm 2.04	24.11 \pm 2.70 ^a
Global SUVR	1.08 \pm 0.06	1.05 \pm 0.20	1.11 \pm 0.15	1.06 \pm 0.17	1.57 \pm 0.18	1.50 \pm 0.17	1.53 \pm 0.17 ^a
Plasma A β_{pE3-40} (fg/mL)	31.00 \pm 16.88	44.59 \pm 30.28	55.41 \pm 28.4	44.09 \pm 28.19	65.64 \pm 18.56	108.2 \pm 63.9	91.62 \pm 54.60 ^a
Plasma A β_{1-40} (pg/mL)	44.65 \pm 9.64	49.39 \pm 7.18	49.53 \pm 8.15	48.57 \pm 7.71	54.28 \pm 6.17	50.28 \pm 6.91	51.84 \pm 6.75
Plasma A β_{pE3-40} -to-A β_{1-40} ratio	(0.072 \pm 0.048)%	(0.092 \pm 0.063)%	(0.108 \pm 0.041)%	(0.091 \pm 0.057)%	(0.122 \pm 0.040)%	(0.215 \pm 0.122)%	(0.179 \pm 0.107)% ^a

Abbreviations: A β , amyloid β ; AD, Alzheimer's disease; aMCI, amnesic mild cognitive impairment; CDR, clinical dementia ranking; Dx, clinical diagnosis; MMSE, mini-mental state examination; NC, normal controls; PET, positron emission tomography; SUVR, standardized uptake value ratio.

^a $P < .05$ between A β PET- and A β PET+; ^{**} $P < .001$ between A β PET- and A β PET+

<2.69%. Hence, the measured A β_{pE3-40} concentration for the spiked 0.1 fg/mL A β_{pE3-40} PBS sample was not counted in Figure 1B. Meanwhile, one of duplicated measurements of IMR(%) for 1000-pg/mL A β_{pE3-40} PBS sample was > 4.46%, which was the upper-limit signal of IMR(%). The measured A β_{pE3-40} concentration was not available for this IMR(%) >4.46%. Hence, the measured A β_{pE3-40} concentration for the spiked 1000-pg/mL A β_{pE3-40} PBS sample was not counted in Figure 1B either. The measured A β_{pE3-40} concentrations versus the spiked A β_{pE3-40} concentrations from 1 fg/mL to 100 pg/mL was plotted in Figure 1B. The slope of the linearity in Figure 1B was found to be 1.07. According to the Clinical & Laboratory Standards Institute (CLSI) guideline EP06-A2, the acceptable range of the slope is from 0.9 to 1.1 for demonstrating the linearity between the measured concentrations and spiked concentrations. Therefore, by taking the results in Figures 1A and 1B into account, the measurement range of A β_{pE3-40} using IMR was from 5 fg/mL to 100 pg/mL.

3.4 | Interference tests of assaying A β_{pE3-40}

Six human plasma samples were prepared for the interference tests, as tabulated in Table 1. Sample No. 1 was native human plasma. Sample No. 2 contained spiked A β_{pE3-40} of 0.05 pg/mL. In addition to 0.05 pg/mL A β_{pE3-40} , Sample No. 3-6 contained difference spiked A β_{3-40} (AS-61029, Anaspec), A β_{1-42} (A9810, Sigma), or A β_{1-40} (A1075, Sigma). It has been reported that the concentration of plasma A β_{1-42} is around 10~20 pg/mL, while plasma A β_{1-40} is 30 to 60 pg/mL.^{24,25,33,34} The spiked A β_{1-42} and A β_{1-40} concentrations in Samples No. 4 through 6 were thus reasonable. The measured A β_{pE3-40} concentrations for each sample are listed in Table 1. The measured A β_{pE3-40} concentration of Sample No. 2 was used as a reference. The recovery rates in the measured A β_{pE3-40} concentrations for Samples No. 3 through 6 were calculated as the ratio of mean concentrations of duplicated measurements for each sample to that of Sample No. 2. The results are shown in Table 1. It was found that the recovery rates for Samples No.

3 through 5 were within the range from 90% to 110%, which means that there was no significant interference to the assay of A β_{pE3-40} in Samples No. 3 through 5. However, the recovery rate of Sample No. 6 was > 110%, which revealed that the 100-pg/mL A β_{1-40} contributed significantly to false signal for assaying A β_{pE3-40} in human plasma. Fortunately, the measured A β_{1-40} concentrations in human plasma were < 100 pg/mL in both healthy controls and AD patients, that is, 30 to 60 pg/mL.^{33,34} Hence, for real human plasma, there would be no significant interferences by A β_{3-40} , A β_{1-42} , or A β_{1-40} to the assay of A β_{pE3-40} using A β_{pE3-40} IMR reagent.

3.5 | Demographic characteristics of enrolled subjects

Forty-six human plasma samples from Taiwan Alzheimer's Disease Neuroimaging Initiative (T-ADNI) were assayed with A β_{pE3-40} IMR reagent. The demographic characteristics, including sex, age, education, APOE ϵ 4 status, CDR, MMSE, global SUVR, and measured plasma A β_{pE3-40} and A β_{1-40} concentrations, are shown in Table 2. In Table 2, the demographic characteristics of various diagnostic groups, that is, normal controls (NC), aMCI, and AD, in A β PET- and A β PET+ are also listed. The combined includes NC, aMCI, and AD. The typical A β PET images of enrolled subjects are shown in Figure 2. Figures 2A-2C are for A β PET- and Figures 2D and 2E are for A β PET+.

The comparisons in the demographic characteristics between A β PET- and A β PET+ individuals, that is, demographic characteristics in combined columns, were made. The age, education years, and CDR between A β PET- and A β PET+ individuals were matched. There was no significant difference in CDR between A β PET- and A β PET+ individuals. The frequency of APOE ϵ 4 allele is much higher in A β PET+ (25%) as compared to A β PET- (7.69%) individuals. Meanwhile, significantly higher scores of MMSE ($P < .001$), higher values of global SUVR ($P < .001$), and higher levels of measured plasma A β_{pE3-40} ($P < .05$) were found in A β PET+ individuals. As to plasma A β_{1-40}

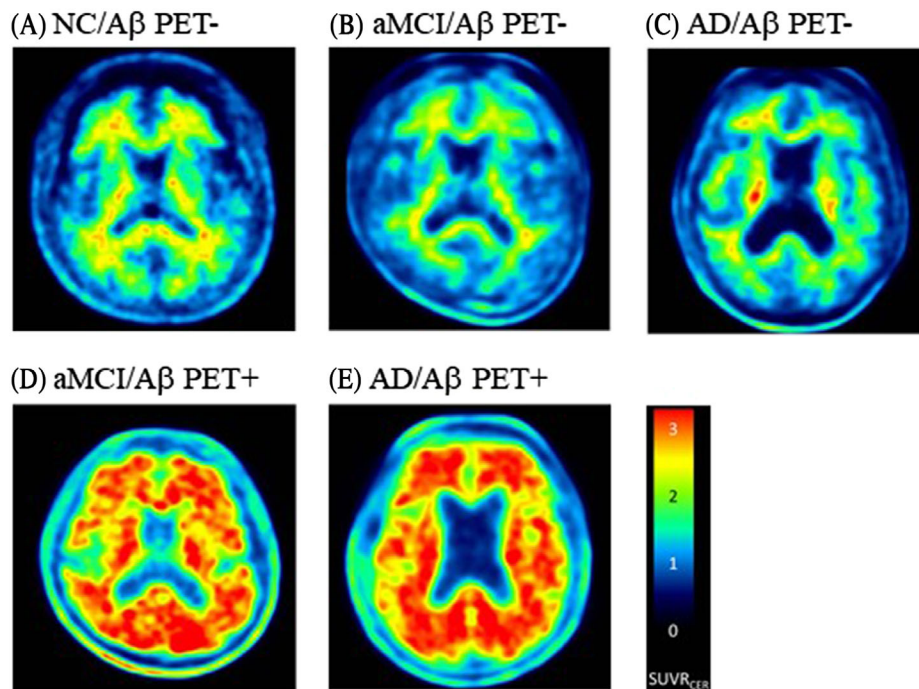


FIGURE 2 Typical amyloid β ($A\beta$) positron emission tomography (PET) images of the enrolled subjects with (A) normal controls (NC) and $A\beta$ PET-, (B) amnesic mild cognitive impairment (aMCI) and $A\beta$ PET-, (C) Alzheimer's disease (AD) and $A\beta$ PET-, (D) aMCI and $A\beta$ PET+, and (E) AD and $A\beta$ PET+

concentrations, there is no significant difference between $A\beta$ PET- and $A\beta$ PET+ individuals.

3.6 | Plasma $A\beta_{pE3-40}$ for discriminating $A\beta$ PET status

The measured plasma $A\beta_{pE3-40}$ concentrations in $A\beta$ PET- and in $A\beta$ PET+ individuals are plotted in Figure 3A. The error bar of each data point in Figure 3A is attributed from the duplicated measurements of plasma $A\beta_{pE3-40}$ concentrations. Concentrations of plasma $A\beta_{pE3-40}$ was 44.1 ± 28.2 fg/mL in $A\beta$ PET- subjects, as compared with 91.6 ± 54.6 fg/mL in the $A\beta$ PET+ group ($P = .012$). The analysis of the receiver operating characteristic (ROC) curve was performed for the data shown in Figure 3A. The ROC curve is shown Figure 3B. The cutoff value of plasma $A\beta_{pE3-40}$ concentration for discriminating $A\beta$ PET- from $A\beta$ PET+ individuals was 56.3 fg/mL, as plotted with the gray dashed line in Figure 3A. The corresponding clinical sensitivity and specificity was 79.0% and 71.4%, respectively. The area under the curve (AUC) was 0.808.

3.7 | Correlation between plasma $A\beta_{pE3-40}$ and SUVR

The relationship between measured plasma $A\beta_{pE3-40}$ concentration and global SUVR is shown in Figure 3C. Through Pearson correlation analysis, the correlation coefficient r was found to be 0.450 ($P < .05$), as guided with the gray dashed line in Figure 3C.

4 | DISCUSSION

Although $A\beta$ PET is approved for diagnosing AD in clinics, it is a very costly and not that accessible of an examination. It would be better to have a screening tool for evaluating the requirement of performing $A\beta$ -PET examination, such as a blood test. Many research groups have tried to develop methods to quantify plasma $A\beta$ in a manner that correlates with $A\beta$ PET. Table 3 lists some typical results showing the possibilities to discriminate $A\beta$ PET- from PET+ using human plasma $A\beta$ species, with $A\beta_{1-40}$ and $A\beta_{1-42}$ being the core biomarkers in these studies. Depending on the clinical diagnosis of enrolled subjects, assay methods and plasma biomarkers, the AUC of discriminating $A\beta$ PET- and PET+ ranges from 0.66 to 0.969. However, studies on the role of plasma $A\beta_{pE3-40}$ in differentiating $A\beta$ PET status are currently lacking. To our knowledge, this is the first study to report the feasibility of discriminating $A\beta$ PET- and PET+ by using plasma $A\beta_{pE3-40}$ in humans. The AUC of 0.808 suggests that $A\beta_{pE3-40}$ in plasma is a promising test for detecting $A\beta$ PET+, which may be of value for screening and diagnosis as well as for applications in longitudinal clinical research studies and to monitor treatments in clinical trials.

The dependence of plasma $A\beta_{pE3-40}$ on $APOE \epsilon 4$ genotype was investigated. There was no significant difference ($P > .05$) in the levels of plasma $A\beta_{pE3-40}$ between $APOE \epsilon 4$ non-carriers (56.58 ± 44.24 fg/mL) and carriers (80.00 ± 49.92 fg/mL), which resonates well with the fact that $A\beta_{pE3-40}$ is generated from $A\beta_{1-40}$ via truncation and pyroglutamation; a process not directly related to $APOE$ genotype. There was no significant difference in levels of plasma $A\beta_{1-40}$ between $A\beta$ PET- and PET+ individuals, but the levels of plasma $A\beta_{pE3-40}$ in $A\beta$

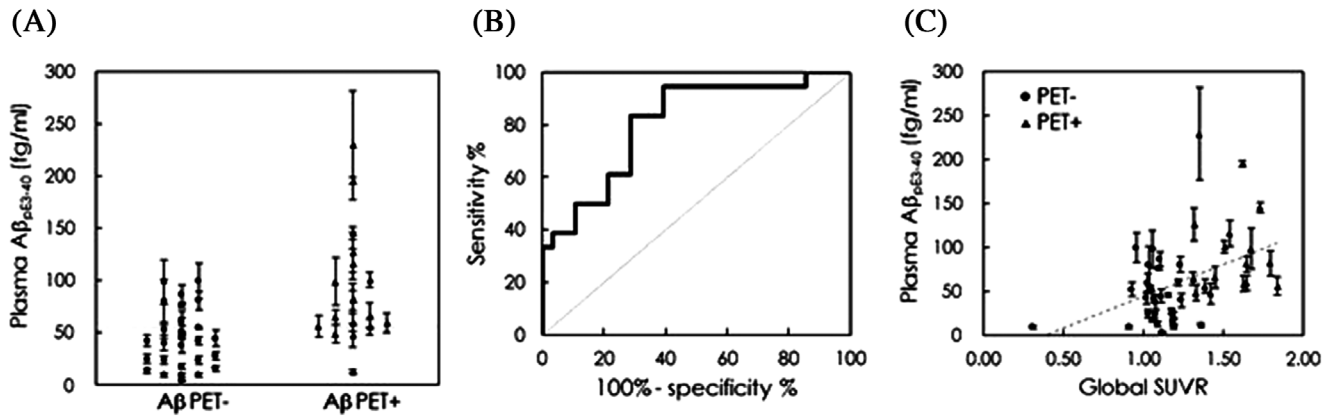


FIGURE 3 (A) Measured concentrations of plasma amyloid β ($A\beta_{pE3-40}$) in $A\beta$ -positron emission tomography (PET)- and $A\beta$ -PET+ subjects using immunomagnetic reduction and (B) receiver operating characteristic (ROC) curve for differentiating PET- from PET+, (C) correlation between measured concentrations of plasma $A\beta_{pE3-40}$ and global standardized uptake value ratio

TABLE 3 Reported plasma $A\beta$ biomarkers for differentiating $A\beta$ PET- from PET+ in AD

References	Dx	N	Assay	Plasma biomarker	$A\beta$ PET- vs. $A\beta$ PET+				P
					Cutoff value	Sensitivity	Specificity	AUC	
37	NC	76	Sandwich ELISA	$A\beta_{1-42}/A\beta_{1-40}$	—	71%	78%	0.79	—
38	SCD	200	Sandwich ELISA	$A\beta_{1-42}/A\beta_{1-40}$	0.08	83.3%	51.9%	0.68	—
39	NC + MCI	39	Sandwich ELISA	$A\beta_{1-40}$	—	—	—	—	.04
				$A\beta_{1-42}/A\beta_{1-40}$	—	—	—	—	.02
40	SCD	69	SIMOA	$A\beta_{1-40}$	—	—	—	0.66	.018
				$A\beta_{1-42}/A\beta_{1-40}$	—	70%	78%	0.79	—
41	NC + MCI + AD	66	IP-MS	$A\beta_{1-42}$	0.183 pg/mL	0.825	0.773	0.808	—
				$A\beta_{1-42}/A\beta_{1-40}$	0.009	0.750	0.773	0.798	—
				$APP669-711/A\beta_{1-42}$	0.914	0.925	0.955	0.969	—
30	NC + MCI + AD	45	IMR	$A\beta_{1-42}/A\beta_{1-40}$	—	—	—	—	< .001
This work	NC + aMCI + AD	46	IMR	$A\beta_{pE3-40}$	55.45 fg/mL	83.3%	71.4%	0.808	.0012

Abbreviations: $A\beta$, amyloid β ; AD, Alzheimer's disease; aMCI, amnesic mild cognitive impairment; AUC, area under curve; ELISA, enzyme-linked immunosorbent assay; IMR, immunomagnetic reduction; IP-MS, immunoprecipitation mass spectrometry; MCI, mild cognitive impairment; NC, normal controls; PET, positron emission tomography; SCD, subjective cognition decline; SIMOA, single molecule array

PET+ subjects were higher, suggesting that $A\beta_{pE3-40}$ is more crucial than $A\beta_{1-40}$ to the formation of $A\beta$ plaques in the brain. The result is corroborated by the plasma $A\beta_{pE3-40}$ -to- $A\beta_{1-40}$ ratio, which was significantly higher ($P < .05$) in $A\beta$ PET+ ($0.179\% \pm 0.107\%$) as compared to $A\beta$ PET- individuals ($0.091\% \pm 0.057\%$).

The roles of plasma $A\beta_{pE3-40}$ in determining cognitive-disorder severity are investigated. As listed in Table 2, for $A\beta$ PET- individuals, MMSE significantly decreases from NC to aMCI and AD ($P < .001$). An obviously different degree of severity in cognitive disorder among diagnostic groups was evidenced in $A\beta$ PET- individuals. Although the mean value of plasma $A\beta_{pE3-40}$ concentrations increases from NC (31.00 fg/mL), aMCI (44.59 fg/mL) to AD (55.41 fg/mL) for $A\beta$ PET- individuals, there is no significant difference among these diagnostic groups. This might be due to the limited range for plasma $A\beta_{pE3-40}$ concentrations in $A\beta$ PET- individuals (44.09 ± 28.19 fg/mL). However, for $A\beta$ PET+ individuals, the plasma $A\beta_{pE3-40}$ concentrations distribute

much more heterogeneously (91.62 ± 54.60 fg/mL) as compared to that for $A\beta$ PET- individuals, as shown in Figure 3A. It might be possible to find the significant difference in the plasma $A\beta_{pE3-40}$ concentrations between aMCI and AD in $A\beta$ PET+ individuals. As tabulated in Table 2, AD with $A\beta$ PET+ shows significantly higher levels of plasma $A\beta_{pE3-40}$ (108.2 ± 63.9 fg/mL) than that of aMCI (65.64 ± 18.56 fg/mL, $P < .05$) with $A\beta$ PET+. These results reveal that plasma $A\beta_{pE3-40}$ level is not only promising to discriminate $A\beta$ PET status, but also able to determine the severity of cognitive disorder in $A\beta$ PET+ individuals.

As expected, the concentration of $A\beta_{pE3-40}$ in human plasma was very low. With the development of ultra-sensitive assays like IMR, it becomes feasible to precisely detect such low concentrations of biomarkers in human plasma. More investigations in plasma $A\beta_{pE3-40}$ shall be explored using ultra-sensitive assays in the future.

There are some limitations in this work. For example, the total number of enrolled subjects is relatively limited. More subjects should be

enrolled for validating the cutoff value of plasma $A\beta_{pE3-40}$ to discriminate $A\beta$ PET status in future studies. Moreover, we did not enroll any pre-clinical AD subject, that is, subjects with normal cognition but $A\beta$ PET+. It would be an important issue to explore the feasibility of using plasma $A\beta_{pE3-40}$ for screening pre-clinical subjects.

5 | CONCLUSION

Reagent for assaying plasma $A\beta_{pE3-40}$ by using immunomagnetic reduction were developed. The measurement range of assaying $A\beta_{pE3-40}$ was 5 fg/mL to 100 pg/mL. The levels of plasma $A\beta_{pE3-40}$ were found to be able to discriminate $A\beta$ PET status. The cutoff value of plasma $A\beta_{pE3-40}$ for discriminating PET- from PET+ was 55.5 fg/mL, showing the sensitivity of 83.3%, specificity of 71.4%, and area under curve of 0.808. Moreover, plasma $A\beta_{pE3-40}$ level is promising to determine the severity of cognitive disorder in $A\beta$ PET+ individuals. As compared to the native primary structure of $A\beta_{1-40}$, the pyroglutamate modification was more closely related to $A\beta$ pathology in the brain. It was also found that $A\beta_{pE3-40}$ is independent of ApoE genotype.

ACKNOWLEDGMENTS

Thank you to Paul Weinreb, Fang Qian, and Robert Scannevin at Biogen Inc. for work in developing the antibodies against $A\beta_{pE3-40}$. Kaj Blennow holds the Torsten Söderberg Professorship in Medicine at the Royal Swedish Academy of Sciences, and is supported by the Swedish Research Council (#2017-00915), the Swedish Alzheimer Foundation (#AF-742881), Hjärfonden, Sweden (#FO2017-0243), and a grant (#ALFGBG-715986) from the Swedish state under the agreement between the Swedish government and the County Councils, the ALF-agreement.

CONFLICTS OF INTEREST

Huei-Chun Liu is an employee of MagQu Co., Ltd. Shieh-Yueh Yang is an employee of MagQu Co., Ltd. and MagQu LLC. Shieh-Yueh Yang is a share owner of MagQu Co., Ltd. Kaj Blennow has served as a consultant, at advisory boards, or given lectures and chairing symposia for Alector, Biogen, CogRx, Lilly, MagQu, Novartis, and Roche Diagnostics, and is a co-founder of Brain Biomarker Solutions in Gothenburg AB, a GU Venture-based platform company at the University of Gothenburg, all unrelated to the work presented in this paper.

REFERENCES

- Hardy JA, Higgins GA. Alzheimer's disease: the amyloid cascade hypothesis. *Science*. 1992;256:184-185.
- Hyman BT, Phelps CH, Beach TG, et al. National Institute on Aging-Alzheimer's Association guidelines for the neuropathologic assessment of Alzheimer's disease. *Alzheimers Dement*. 2012;8:1-13.
- Leinonen V, Koivisto AM, Savolainen S, et al. Amyloid and tau proteins in cortical brain biopsy and Alzheimer's disease. *Ann Neurol*. 2010;68:446-453.
- Masters CL, Bateman R, Blennow K, Rowe CC, Sperling RA, Cummings JL. Alzheimer's disease. *Nat Rev Dis Primers*. 2015;1:15056.
- Pike CJ, Overman MJ, Cotman CW. Amino-terminal deletions enhance aggregation of beta-amyloid peptides in vitro. *J Biol Chem*. 1995;270:23895-23898.
- Liu K, Solano I, Mann D, et al. Characterization of Abeta11-40/42 peptide deposition in Alzheimer's disease and young Down's syndrome brains: implication of N-terminally truncated Abeta species in the pathogenesis of Alzheimer's disease. *Acta Neuropathol*. 2006;112:163-174.
- Piccini A, Russo C, Gliozzi A, et al. beta-amyloid is different in normal aging and in Alzheimer disease. *J Biol Chem*. 2005;280:34186-34192.
- Mori H, Takio K, Ogawara M, Selkoe DJ. Mass spectrometry of purified amyloid beta protein in Alzheimer's disease. *J Biol Chem*. 1992;267:17082-17086.
- Harigaya Y, Saido TC, Eckman CB, Prada CM, Shoji M, Younkin SG. Amyloid beta protein starting pyroglutamate at position 3 is a major component of the amyloid deposits in the Alzheimer's disease brain. *Biochem Biophys Res Commun*. 2000;276:422-427.
- Portelius E, Bogdanovic N, Gustavsson MK, et al. Mass spectrometric characterization of brain amyloid beta isoform signatures in familial and sporadic Alzheimer's disease. *Acta Neuropathol*. 2010;120:185-193.
- Saido TC, Yamao-Harigaya W, Iwatsubo T, Kawashima S. Amino- and carboxyl-terminal heterogeneity of beta-amyloid peptides deposited in human brain. *Neurosci Lett*. 1996;215:173-176.
- Russo C, Salis S, Dolcini V, et al. Amino-terminal modification and tyrosine phosphorylation of [corrected] carboxy-terminal fragments of the amyloid precursor protein in Alzheimer's disease and Down's syndrome brain. *Neurobiol Dis*. 2001;8:173-180.
- Schilling S, Lauber T, Schaupp M, et al. On the seeding and oligomerization of pGlu-amyloid peptides (in vitro). *Biochemistry*. 2006;45:12393-12399.
- Saido TC, Iwatsubo T, Mann DM, Shimada H, Ihara Y, Kawashima S. Dominant and differential deposition of distinct beta-amyloid peptide species, A beta N3(pE), in senile plaques. *Neuron*. 1995;14:457-466.
- Hosoda R, Saido TC, Otvos L, Jr., et al. Quantification of modified amyloid beta peptides in Alzheimer disease and Down syndrome brains. *J Neuropathol Exp Neurol*. 1998;57:1089-1095.
- Wirhth O, Bethge T, Marcello A, et al. Pyroglutamate Abeta pathology in APP/PS1KI mice, sporadic and familial Alzheimer's disease cases. *J Neural Transm*. 2010;117:85-96.
- Frost JL, Le KX, Cynis H, et al. Pyroglutamate-3 amyloid-beta deposition in the brains of humans, non-human primates, canines, and Alzheimer disease-like transgenic mouse models. *Am J Pathol*. 2013;183:369-381.
- Mandler M, Rockenstein E, Ubhi K, et al. Detection of peri-synaptic amyloid-beta pyroglutamate aggregates in early stages of Alzheimer's disease and in AbetaPP transgenic mice using a novel monoclonal antibody. *J Alzheimers Dis*. 2012;28:783-794.
- Schmidt F, Boltze J, Jager C, et al. Detection and quantification of beta-Amyloid, pyroglutamyl Abeta, and Tau in aged canines. *J Neuropathol Exp Neurol*. 2015;74:912-923.
- Sergeant N, Bombois S, Ghestem A, et al. Truncated beta-amyloid peptide species in pre-clinical Alzheimer's disease as new targets for the vaccination approach. *J Neurochem*. 2003;85:1581-1591.
- Maeda J, Ji B, Irie T, et al. Longitudinal, quantitative assessment of amyloid, neuroinflammation, and anti-amyloid treatment in a living mouse model of Alzheimer's disease enabled by positron emission tomography. *J Neurosci*. 2007;27:10957-10968.
- Cheih JJ, Yang SY, Horng HE, et al. Immunomagnetic reduction assay using high-Tc superconducting-quantum-interference-device-based magnetosusceptometry. *J Appl Phys*. 2010;107:074903.
- Huang KW, Yang SY, Yu CY, et al. Exploration of the relationship between the tumor burden and the concentration of vascular endothel-

- lial growth factor in liver-cancer-bearing animals using immunomagnetic reduction assay. *J Biomed Nanotechnol.* 2011;7:535-541.
24. Teunissen CE, Chiu MJ, Yang CC, et al. Plasma Amyloid-beta (Abeta42) correlates with cerebrospinal fluid Abeta42 in Alzheimer's disease. *J Alzheimers Dis.* 2018;62:1857-1863.
 25. Tzen KY, Yang SY, Chen TF, et al. Plasma Abeta but not tau is related to brain PiB retention in early Alzheimer's disease. *ACS Chem Neurosci.* 2014;5:830-836.
 26. Fan LY, Tzen KY, Chen YF, et al. The relation between brain amyloid deposition, cortical atrophy, and plasma biomarkers in amnesic mild cognitive impairment and Alzheimer's disease. *Front Aging Neurosci.* 2018;10:175.
 27. Yang SY, Jian ZF, Horng HE, et al. Dual immobilization and magnetic manipulation of magnetic nanoparticles. *J Magn Magn Mater.* 2008;320:2688-2691.
 28. McKhann GM, Knopman DS, Chertkow H, et al. The diagnosis of dementia due to Alzheimer's disease: recommendations from the National Institute on Aging-Alzheimer's Association workgroups on diagnostic guidelines for Alzheimer's disease. *Alzheimers Dement.* 2011;7:263-269.
 29. Emi M, Wu LL, Robertson MA, et al. Genotyping and sequence analysis of apolipoprotein E isoforms. *Genomics.* 1988;3:373-379.
 30. Lin KJ, Hsu WC, Hsiao IT, et al. Whole-body biodistribution and brain PET imaging with [¹⁸F]AV-45, a novel amyloid imaging agent—a pilot study. *Nucl Med Biol.* 2010;37:497-508.
 31. Hsiao IT, Huang CC, Hsieh CJ, et al. Perfusion-like template and standardized normalization-based brain image analysis using 18F-florbetapir (AV-45/Amyvid) PET. *Eur J Nucl Med Mol Imaging.* 2013;40:908-920.
 32. Johnson KA, Sperling RA, Gidicsin CM, et al. Florbetapir (F18-AV-45) PET to assess amyloid burden in Alzheimer's disease dementia, mild cognitive impairment, and normal aging. *Alzheimers Dement.* 2013;9:S72-83.
 33. Chiu MJ, Yang SY, Horng HE, et al. Combined plasma biomarkers for diagnosing mild cognition impairment and Alzheimer's disease. *ACS Chem Neurosci.* 2013;4:1530-1536.
 34. Lue LF, Sabbagh MN, Chiu MJ, et al. Plasma levels of Abeta42 and Tau identified probable Alzheimer's dementia: findings in two cohorts. *Front Aging Neurosci.* 2017;9:226.
 35. Fandos N, Perez-Grijalba V, Pesini P, et al. Plasma amyloid beta 42/40 ratios as biomarkers for amyloid beta cerebral deposition in cognitively normal individuals. *Alzheimers Dement.* 2017;8:179-87.
 36. de Rojas I, Romero J, Rodriguez-Gomez O, et al. Correlations between plasma and PET beta-amyloid levels in individuals with subjective cognitive decline: the Fundacio ACE Healthy Brain Initiative (FACEHBI). *Alzheimers Res Ther.* 2018;10:119.
 37. Devanand DP, Schupf N, Stern Y, et al. Plasma Abeta and PET PiB binding are inversely related in mild cognitive impairment. *Neurology.* 2011;77:125-131.
 38. Verberk IMW, Slot RE, Verfaillie SCJ, et al. Plasma amyloid as prescreener for the earliest Alzheimer pathological changes. *Ann Neurol.* 2018;84:648-658.
 39. Kaneko N, Nakamura A, Washimi Y, et al. Novel plasma biomarker surrogating cerebral amyloid deposition. *Proc Jpn Acad Ser B Phys Biol Sci.* 2014;90:353-364.

How to cite this article: Wang P-N, Lin K-J, Liu H-C, et al. Plasma pyroglutamate-modified amyloid beta differentiates amyloid pathology. *Alzheimer's Dement.* 2020;12:e12029. <https://doi.org/10.1002/dad2.12029>